SIMULATION OF EXPERIMENT ON LIGHT GAS LAYER EROSION IN SMALL-SCALE MCTHBF CONTAINMENT EXPERIMENTAL FACILITY

Rok Krpan, Ivo Kljenak*
Jozef Stefan Institute
Jamova cesta 39, SI-1000 Ljubljana, Slovenia
rok.krpan@ijs.si, ivo.kljenak@ijs.si

Houjun Gong, Ying Wang, Yuanfeng Zan, Pengzhou Li
Nuclear Power Institute of China
P.O.Box 622-205 Chengdu, Sichuan Province, P.R. China 610213
ghjtsing@126.com, 88366322@qq.com, yfzan@163.com, pengzhouli@aliyun.com

Etienne Studer
Commissariat à l'Energie Atomique et aux Energies Alternatives
DEN/DM2S/SFME/LATF, CEA Saclay, F-91191 Gif-sur-Yvette, France
etienne.studer@cea.fr

Ahmed Bentaïb
Institut de Radioprotection et de Sûreté Nucléaire
31, Avenue de la division Leclerc, F-92262 Fontenay-aux-Roses, France
ahmed.bentaib@irsn.fr

Namane Méchitoua
Electricité de France Research and Development
6, Quai Watier, F-78401 Chatou, France
namane.mechitoua@edf.fr

ABSTRACT

An experiment on mixing of stratified atmosphere in the containment, induced by vertical air injection, was simulated with the Computational Fluid Dynamics (CFD) code OpenFoam. The experiment was performed in the MCTHBF test facility (Mid-scale Containment Thermal Hydraulic - Hydrogen Behaviour Test Facility) at the Nuclear Power Institute of China (NPIC) in Chengdu (P.R. China). The experiment, in which the erosion of a horizontal helium layer occurred, replicated the eventual decrease of high local hydrogen concentration due to gas flow within the containment atmosphere. A three-dimensional numerical model of the cylindrical MCTHBF vessel was developed. Simulation results of helium concentration at different locations are compared to experimental data. Contrary to the experiment, in which the layer erosion occurred homogeneously within the layer, the simulation predicted a non-homogeneous erosion.

KEYWORDS
Containment, Mixing, Hydrogen

* Corresponding author

1. INTRODUCTION

Hydrogen risk is one of the issues in research on severe accidents in light water reactor nuclear power plants [1]. Namely, hydrogen would be generated due to the oxidation of the reactor core during a severe accident and would flow into the containment. Due to possible non-homogeneous distribution, local hydrogen concentration in some regions of the containment could exceed the flammability limit in an air-steam-hydrogen gaseous mixture, leading to combustion caused by some random ignition (which should always be assumed). This scenario occurred during the Three Mile Island accident in the USA in 1979, but the combustion pressure peak was still lower than the containment design pressure. Hydrogen combustion also occurred during the Fukushima accident in Japan in 2011, except that the two visible explosions occurred in the reactor auxiliary building that was not designed for such pressure spikes in the first place.

One of the investigated phenomena is the mixing of the atmosphere in the containment, induced by some gaseous flow. Namely, the high local concentration of hydrogen in a non-homogeneous containment atmosphere could be decreased by mixing caused by the flow of gas, directly or indirectly induced by the flow from the break of the reactor coolant system. This flow could be either low-momentum (plume or jet) or high-momentum (jet). These investigations include experiments performed in containment experimental facilities, using helium as a substitute gas for hydrogen for safety reasons. One such experiment was performed in 2018 within the Chinese-European project ALISA (Access to Large Infrastructures for Severe Accidents) at the Nuclear Power Institute of China (NPIC) in Chengdu (P.R. China) in the MCTHBF test facility (Mid-scale Containment Thermal Hydraulic - Hydrogen Behaviour Test Facility). The main part of the MCTHBF facility is a cylindrical vessel with a volume of 21 m^3. In the experiment, a horizontal gas layer with high helium concentration was established first in the vessel upper part. Then, a vertical jet of air was injected from the vessel lower part during one hour. The experiment replicated the decrease of high local hydrogen concentration due to mixing induced by the gas flow within the containment atmosphere.

To devise successful mitigation measures of high hydrogen concentration in the containment, accurate and reliable simulations on the local instantaneous scale of the non-homogeneous containment atmosphere behaviour are beneficial. Although the containment volumes of actual nuclear power plants are much too large for simulations that would replicate longer transients (that is, of the order of a few hours at least), models included in Computational Fluid Dynamics (CFD) codes are still being developed and validated in the hope that they will some day be useful for such simulations. These developments and validations are being done by comparing simulation results with measured data from experiments, mentioned above. Models developed in such a way should in principle be also adequate for actual nuclear containments, although their volumes are some three orders of magnitude larger than volumes of experimental vessels. Namely, the length scale of key phenomena (presumably turbulent flow and buoyancy), which have a decisive influence on the mixing of the containment atmosphere, is at least an order of magnitude lower that the volume of experimental vessels, if not even lower. Thus, the larger volume encompassing the portion of the space where the key phenomena occur should have no influence on the local processes.

In the present paper, the above-mentioned experiment performed in the MCTHBF facility was simulated with the CFD code OpenFoam. The simulation is part of a wider project to develop an adequate modelling approach (that is, selection of specific models, development of numerical grids, specific modelling of gas injection) to successfully simulate such experiments. The OpenFoam code was selected as it is an open-source code, which offers wider perspectives for the future development and implementation of new or improved models. Basically, initial and boundary conditions were prescribed from the experiment specification. However, after the first simulations produced some results with some notable differences from measured data, these conditions were also varied within experimental uncertainties to try to improve the agreement between simulation and experimental results.

2. EXPERIMENTAL FACILITY

MCTHBF is a midsize containment thermal hydraulic hydrogen mitigation test facility. The layout of the facility, with all the necessary devices to establish and maintain the prescribed experimental conditions, is shown schematically in Figure 1. Although the facility was used to perform an experiment on containment atmosphere mixing, it may be used to perform experiments on hydrogen combustion as well.

The main part of the facility is a steel cylindrical vessel, with 5 m height and 2.8 m diameter (Figure 2). The vessel volume is about 21 m^3. The mixed gas content, gas temperature and pressure, and (eventually) flame propagation velocity can be measured using a gas analyser, a thermocouple array and piezoelectric pressure sensors. The vessel can deal with hydrogen concentrations between 0 and 35 vol.% , as well as steam concentrations between 0 and 40 vol.%.

Compared to other vessels used for such experiments on hydrogen distribution, such as the PANDA and MISTRA vessels mentioned later [2], or the THAI facility (operated by Becker Technologies GmbH in Eschborn, Germany), the MCTHBF vessel is much smaller. Among the facilities which were used in the past two decades, only the TOSQAN vessel [3], with a 7 m^3 volume, is smaller. For this reason, the MCTHBF vessel falls within “small-scale” or “medium-scale” facilities. The shape of the MCTHBF vessel is also somewhat different from the shapes of other containment experimental facilities, where the diameter is usually constant almost all the way up until the vessel ceiling. In fact, the shape of the MCTHBF vessel is somewhat reminiscent of the containment of the Fukushima Daiichi nuclear power plant units, which are Boiling Water Reactors built in the 1970-ies. However, the actual containment of these plants did not have such free volumes due to the space taken by the reactor coolant system. Be that as it may, experiments in the MCTHBF facility are an interesting addition to the experimental data base on the topic of containment atmosphere mixing. As to the influence of the different shape on the mixing of the atmosphere, it should not be decisive due to the much lower length scale of key phenomena than the dimensions of the vessel (as already discussed in the introduction).

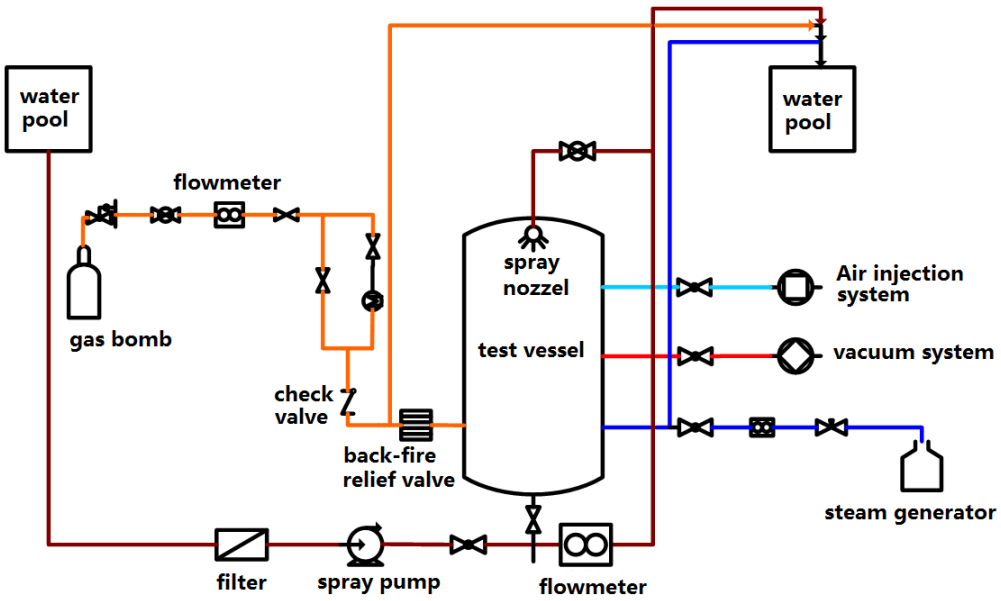

Figure 1. Schematic of the MCTHBF experimental facility.

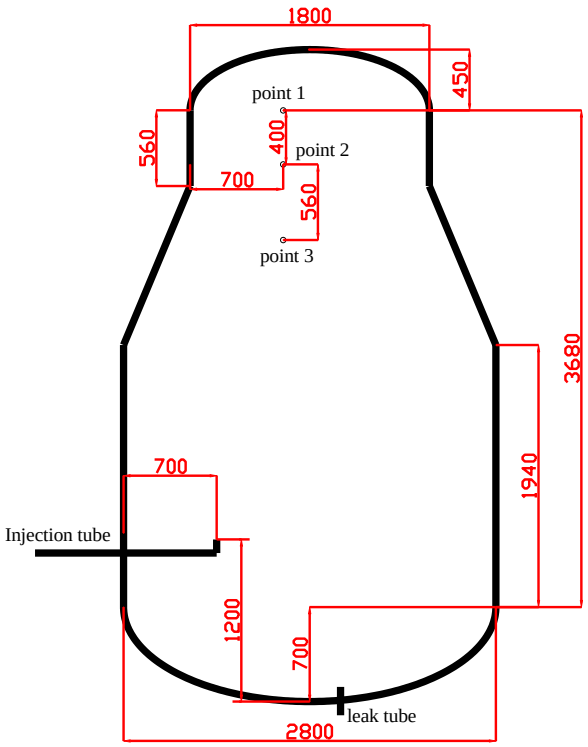

Figure 2. Schematic of the MCTHBF experimental vessel, configured for the presented experiment.

3. EXPERIMENTAL CONDITIONS

The proposed experiment was designed to replicate the eventual decrease of high local hydrogen concentration due to gas flow within the containment atmosphere. Namely, steam released from the reactor coolant system through the eventual break, be it low-momentum (plume or jet) or high-momentum (jet), would either interact directly with an atmosphere region with high-concentration of hydrogen, or would initiate circulation in the containment that would cause atmosphere mixing.

In the experiment, a horizontal gas layer with high helium (that was used as a substitute for hydrogen for safety reasons) concentration was established first in the vessel upper part [4]. Then, a vertical jet of air was injected from the vessel lower part. Although a steam jet is expected during an actual accident, the use of air enables delimiting the effect of the interaction of a gaseous jet with a stratified atmosphere from the additional effects caused by steam condensation. Furthermore, experiments with air are performed at lower temperatures, which minimizes or even eliminates heat losses and the generation of cold gas plumes formed in colder wall regions. Such plumes could in principle have a strong impact on atmosphere mixing, especially in the regions far away from the rising jet.

The interaction of a vertical gas jet with a stratified atmosphere has already been the subject of many previous experimental investigations. Within the OECD SETH-2 project (2007-2010) [2], a number of tests were performed in the MISTRA facility, located at the Commissariat à l'Energie Atomique et aux Energies Alternatives - CEA in Saclay (France) and in the PANDA facility, located at the Paul Scherrer Institute in Villigen (Switzerland). MISTRA is a cylindrical vessel with a volume of 98 m^3, whereas the cylindrical vessel of the PANDA facility that was used has a volume of 90 m^3. In both facilities, a layer of helium was established first in the upper part of the vessel. Then, a vertical upward jet of air was injected below the helium layer, and the subsequent evolution of the helium concentration in the vessel

(that is, the progressive dilution of the layer and the mixing of the helium with the atmosphere below) was observed. Some tests (tests MISTRA LOWMA3 and LOWMA4, and test PANDA ST1-7), were intentionally performed at similar initial and boundary conditions, and the similarities in the observed behaviour of the helium layer were later analysed [5]. Quantitative similarity criteria were also proposed based on the analyses.

The proposed experiment in the MCTHBF facility was designed to be performed at similar conditions as the tests MISTRA LOWMA3 and LOWMA4, and test PANDA ST1-7, with the purpose to obtain experimental data, suitable for scaling results from smaller to larger volumes (although with a basically different shape). Thus, the experiment in the MCTHBF facility provided the opportunity to observe the erosion of a light gas layer at similar pressure and temperature conditions, with a similar air jet (in terms of momentum and mass flow rate), but in a smaller vessel. The experimental scaling-up of the experiment from 21 m^3 (MCTHBF) to 98 m^3 (MISTRA) and 90 m^3 (PANDA) could contribute to the understanding of the scaling-up of specific phenomena, which is a step towards scaling-up to actual nuclear power plant containments. This is not in contradiction with the earlier statements on the non-influence of the vessel size. Namely, the vessel size should not influence local processes, which are described in the basic equations using local instantaneous description, and thus specific physical models should apply to all vessel sizes. However, the overall effect of the local processes could eventually be different in vessels of different sizes.

Table I provides a comparison of the main features between the MISTRA LOWMA3 and LOWMA4, PANDA ST1-7 and MCTHBF experiments.

Table I. Comparison of MISTRA, PANDA and MCTHBF experiments.

Experiment	**MISTRA LOWMA3**	**MISTRA LOWMA4**	**PANDA ST1-7**	**MCTHBF**
Vessel volume (m^3)	98		90	21
Vessel height (mm)	7379		7984	4930
Injection height (mm)	3660		4013	1200
Elevation of layer low. bound. (mm)	5800		4875	3520
Layer height (mm)	1300		1250	1410
Injection diameter (mm)	72		75	32
Injection flow rate (g/s)	4.5	50.6	15	15

The experiment proceeded in the following steps:

1. Establishment of initial pressure and temperature conditions
An air atmosphere at pressure 1 bar and temperature about 20 °C (room temperature) was established in the vessel. The facility had to be opened in order to prevent pressure increase.

2. Establishment of helium layer in the vessel upper part
A helium layer, with a concentration of about 40 vol.%, was established in the upper part of the vessel, 3.5 m – 4 m above the vessel floor. The concentration at measuring points 1, 2, and 3 (Figure 2) was higher than 40 vol.%.

3. Injection of vertical air jet
Air was injected through a vertical tube, with a diameter of 32 mm, during 1 hour, with a mass flow rate of 15 g/s. The injection nozzle was located at 1/4 vessel diameter, and at elevation 1.2 m above the vessel floor.

4. Evolution of the atmosphere

The evolution of the helium concentration in the atmosphere at different locations (measuring points 1, 2, and 3) was observed during the two hours from the start of air injection.

4. EXPERIMENTAL RESULTS

The experimental results of helium concentration are presented in Figure 3. As may be seen in the figure, the established helium horizontal layer was quite homogeneous. The concentration slightly increased with elevation, which could be expected and is almost unavoidable (given the fairly large difference in the elevations of the measuring points: 400 mm and 560 mm, compared to the local vessel diameter: 1800 mm).

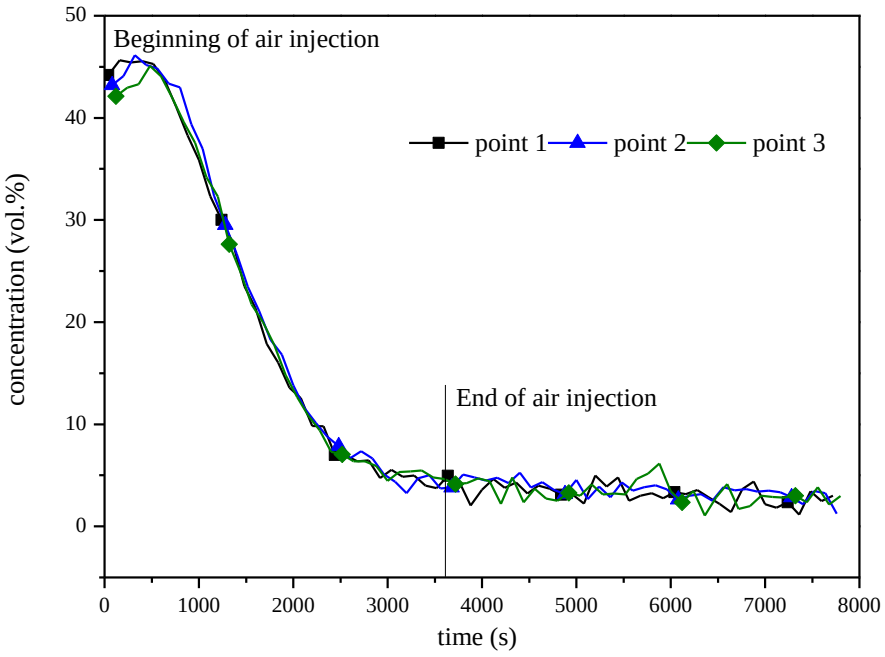

Figure 3. Measured time-dependent helium concentration at different measuring points.

The following characteristic features may be observed after the start of air injection:

— the pattern of the gradual concentration decrease is similar to the one, observed during experiments in the MISTRA and PANDA facilities;
— despite the differences in elevations of the measuring points, the curves are very close, right from the beginning of the air injection.

The similarity of the observed time-dependent behaviour of the helium concentration with the one, observed earlier in the MISTRA and PANDA experimental facilities, could be expected. First, although the MISTRA and PANDA vessels are much larger, they are still of the same order of magnitude. Second, the experimental conditions were prescribed, based on the similarity criteria developed in ref. [5], so that the results would be qualitatively similar.

The closeness of the curves, related to different measuring points, is a more interesting feature. First of all, three periods should be differentiated (based on observed results and execution of experiment):

— time interval during air injection, before helium concentration drops to about 7.5 vol.%,
— time interval during air injection, after helium concentration drops to about 7.5 vol.%,
— time interval after air injection is stopped.

During the first time interval, the curves are very close, almost overlapping. This shows, that the mixing occurred with the same intensity over the helium layer thickness right from the beginning, without a gradual erosion. This is a phenomenon that was not observed in the PANDA and MISTRA experiments. This could be an indication, that the jet air mass flow rate, prescribed based on similarity criteria proposed in ref. [5], was too high for the prescribed vertical distance between the outlet of the injection tube and the lower boundary of the helium layer (that is, too high if similar mixing as in the PANDA and MISTRA facility had to be achieved). Another possibility is that the high helium concentration layer extended towards the vessel bottom significantly lower than the lowest measuring location.

After the helium concentration drops to about 7.5 vol.%, the curves do not overlap so much, despite the continuation of air injection during about 1100 s. It seems that, at this stage, the helium layer becomes less homogeneous. This is quite an interesting feature, because one would expect the opposite: that the helium layer would stay all the more homogeneous at low concentration (given that air is still being injected). This feature should be investigated further before explanations are proposed. Also, measurement uncertainties will have to be evaluated.

Finally, after the air injection is stopped, the curves overlap even less and fluctuate about some averages which are slowly decreasing. The decrease of the averages may be attributed to slow gradual mixing with the rest of the vessel atmosphere, whereas the fluctuations may be attributed to the remaining inertial turbulent motion following the mixing induced by the air injection.

5. THEORETICAL MODELLING

Numerical simulations were performed with the OpenFoam CFD code, version 1606+ [6]. To simulate the transient mixing process, the Unsteady Reynolds Averaged Navier Stokes (URANS) approach was used. An adaptive time step (approx. 0.001 s) was used, to sustain a Courant-Friedrichs-Lewy number of less than 0.5 in all cells. Second-order spatial discretization schemes were used and the temporal term was exceptionally discretized using a first-order differencing scheme.

5.1. Fluid Flow Model

The atmosphere in the vessel was considered as a compressible mixture of perfect gases. The light gas layer erosion and mixing process was modelled as a single-phase flow of two components. The common momentum equation solved was:

$$\frac{\partial \rho U_i}{\partial t} + \frac{\partial}{\partial x_j}\left(\rho U_i U_j\right) = -\frac{\partial p}{\partial x_i} + \frac{\partial}{\partial x_j}\left((\mu + \mu_t)\left(\frac{\partial U_i}{\partial x_j} + \frac{\partial U_j}{\partial x_i}\right)\right) - g_k x_k \frac{\partial \rho}{\partial x_i} \quad (1)$$

where ρ, t, U, p, μ, μ_t and g are density, time, velocity, pressure, dynamic and eddy viscosity, and gravitational acceleration, respectively. The solved energy equation was:

$$\frac{\partial \rho h}{\partial t} + \frac{\partial}{\partial x_j}(\rho U_i h) + \frac{\partial \rho K}{\partial t} + \frac{\partial}{\partial x_j}(\rho U_i K) - \frac{\partial p}{\partial t} = \frac{\partial}{\partial x_j}\left(\left(\frac{\mu}{Pr} + \frac{\mu_t}{Pr_t}\right)\frac{\partial h}{\partial x_j}\right) - \frac{\partial q_r}{\partial x_j} + \rho g_k U_k \quad (2)$$

where h, K, Pr, Pr_t and q_r are enthalpy, kinetic energy, Prandtl and turbulent Prandtl number and radiative heat flux, respectively. Included gas species mass fractions were considered as passive scalars. The i-th species mass fraction, Yi, was calculated using the diffusion equation:

$$\frac{\partial \rho Y_i}{\partial t} + \frac{\partial}{\partial x_j}(\rho U_i Y_i) = \frac{\partial}{\partial x_j}\left(\left(\frac{\mu}{Sc} + \frac{\mu_t}{Sc_t}\right)\frac{\partial Y_i}{\partial x_j}\right) \quad (3)$$

where Sc and Sc_t are the Schmidt number and the turbulent Schmidt number, respectively. Physical properties of used gases are listed in Table II.

Table II. Physical properties of included gases

	Helium	Air
***T* (°C)**	20	
***Cp* (kJ/kg)**	5193	1005
***μ* (Ns/m^2)**	0.198 x 10^{-4}	0.182 x 10^{-4}
Pr	0.664	0.713

The turbulent Prandtl number and the turbulent Schmidt number were set to 0.9. Selected values of these numbers gave the best results, when simulating similar experiments with this physical model [11].

The average quantities used in equations above are calculated with the use of mass fractions as:

$$\mu = Y_1\mu_1 + Y_2\mu_2 \tag{4}$$

$$Cp = Y_1Cp_1 + Y_2Cp_2 \tag{5}$$

$$Pr = Y_1Pr_1 + Y_2Pr_2 \tag{6}$$

The Launder and Spalding *k*-ε turbulence model [7] with an additional buoyancy term by Henkes et al. [8], implemented in OpenFoam, was used for turbulence modelling. The reason for selecting this model is that it is intensively studied and improved for buoyant flows, and consequently it is commonly used for simulations of containment atmosphere mixing. Although the initial jet is momentum driven, the light gas layer causes a strong density gradient and negative buoyancy effect that changes the flow direction and also affects the turbulence.

5.2. Radiation Heat Transfer Model

The effect of the heat transfer by radiation was also included in the present work. Namely, radiation is a phenomenon that is often neglected in modelling of containment atmosphere phenomena, although it can have a significant influence. The P-1 radiation model is the lowest order case of the P-N model, which is based on the expansion of the radiation intensity into an orthogonal series of spherical harmonics. The radiation flux, q_r, in Eq. (2) can be written as [9]:

$$q_r = -\frac{1}{3a}\frac{\partial G}{\partial x_j} \tag{7}$$

where *a* and *G* are the absorption coefficient and incident radiation, respectively. The transport equation for *G* is [9]:

$$-\frac{\partial q_r}{\partial x_j} = aG - 4e\sigma_B T^4 \tag{8}$$

where *e,* σ_B and *T* are emission coefficient, Stefan-Boltzmann constant and temperature, respectively. The emission coefficient and absorption coefficient values were set to 0.5. The selected coefficient values gave the best results or did not cause numerical instabilities of the calculations.

The Marshak boundary condition [10] was prescribed for all boundaries (i.e. inlet, outlet, pipe and walls). The boundaries were specified as black bodies with emissivity and absorptivity 1. Any other emissivity or absorptivity values caused numerical errors.

5.3. Computational Mesh and Boundary Conditions

A semi-cylindrical three-dimensional numerical model was developed (Figure 4) without any simplifications of the geometry (Figure 2). The origin of the coordinate system in the domain is located at the bottom of the vertical axis of the vessel. The coordinates *x* and *y* represent the radial (crosswise and spanwise) directions and *z* represents the axial (streamwise) direction.

To better resolve the inflow, the flow near the injection tube, the mixing process and the outflow, the orthogonal mesh was refined above the inlet, in the region with high helium concentration, around the pipe, and near the outlet (Figure 4). The parameters of the mesh used for calculations are listed in Table III. Due to the very long computational time and, as was found during the mesh convergence study performed in ref. [11], very little results improvement, a convergence study was not performed.

Table III. Mesh parameters

N	Δx [cm]	Δy [cm]	Δz [cm]	Max aspect ratio	Non-orthogonality	Max skewness	Expansion ratio
392,483	0.5 - 4	0.5 - 4	0.5 - 4	4.6	48.1 (max), 3.02 (average)	1.92	2

The symmetry boundary condition was prescribed in the central plane. The injection tube was not resolved, and, on the inlet, constant mass flow with constant temperature was prescribed. On the outlet, a zero gradient boundary condition with constant pressure was used. All other patches were prescribed as walls. In ref. [11], it was discussed that wall temperature during experiments performed in the PANDA experimental facility is approximately constant, and, for this reason, a constant wall temperature was prescribed. On the walls, wall functions were prescribed for turbulence quantities and the no-slip boundary condition was prescribed for velocity. Initial conditions in the simulations were prescribed as described in Section 3.

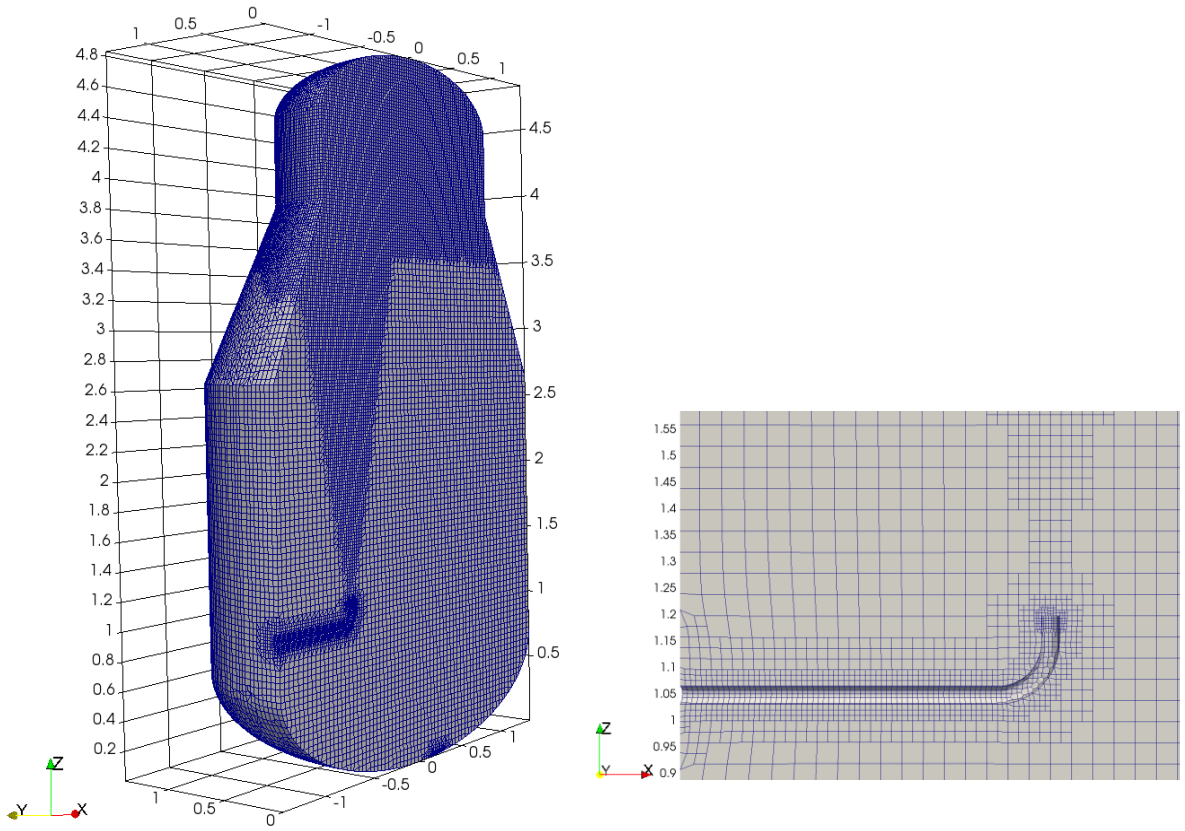

Figure 4. Numerical mesh (left) and refined region around inlet and pipe (right).

6. RESULTS AND DISCUSSION

Only the air injection phase, that is the first 3600 s of the experiment, was simulated.

Three simulations with different initial helium profile were performed (Figure 5). Namely, as already stated, the specific feature of the experimental results is the closeness of the curves showing the gradual decrease of helium concentration at different elevations.

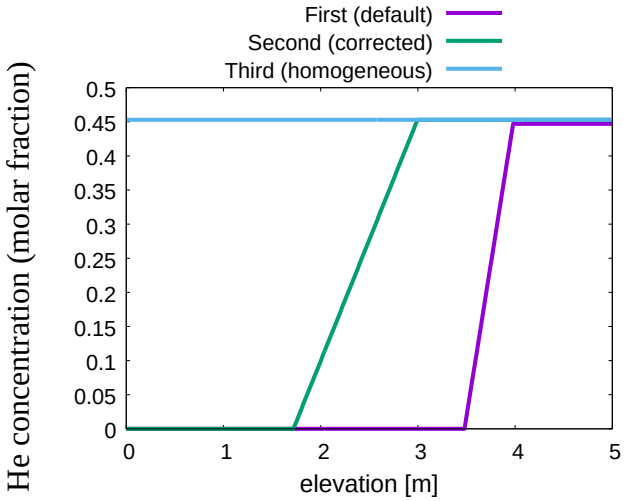

Figure 5. Initial He distribution profiles used in simulations.

6.1. Simulation with Prescribed Experimental Conditions

In the first simulation, the lower boundary of the helium layer was assumed to be just above point 3, located at elevation 3.420 m (Figure 2). In the simulation (Figure 6, in which, due to the very close values measured in different points, experimental results are presented with a single curve), the light gas layer erosion started much sooner and occurred much faster than in the experiment. Also, again contrary to the experiment, in which the layer erosion occurred homogeneously, the simulation predicted a non-homogeneous erosion with a time shift between the curves.

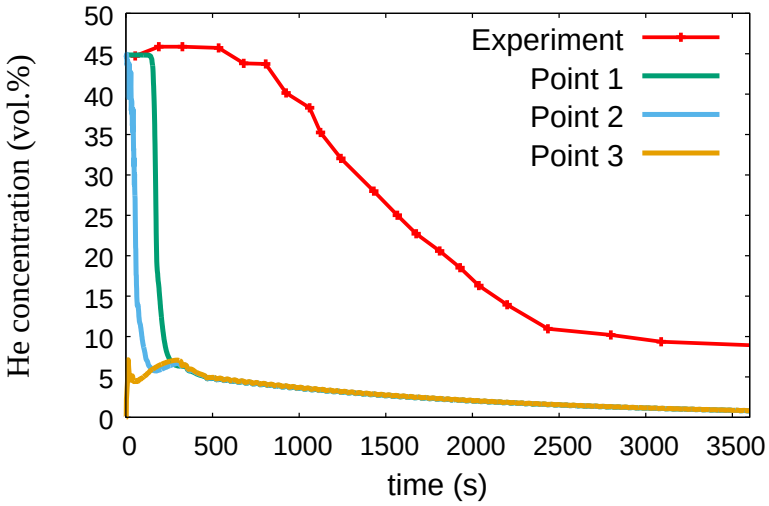

Figure 6. Time-dependent He concentration with default (high) lower boundary of He layer (only a single experimental curve is shown).

6.2. Simulation with Modified Initial Conditions

It was inferred, that a possible reason for the homogeneous erosion in the experiment was that the lower boundary of the helium layer was much lower, but was not detected. For this reason, additional simulations with a corrected (lower) initial boundary of the helium layer were performed. In the second simulation, the initial light gas gradient region was between 1.7 m and 3 m (Figure 5) and the concentration gradient itself was the same as it was in the ST1_7 experiment performed in the PANDA experimental facility [5]. In this simulation, erosion started at first at lowest point 3 and the latest at the highest point 1 (Figure 7). It can be also observed that the time interval between the start of the erosion at different elevations is somewhat shorter.

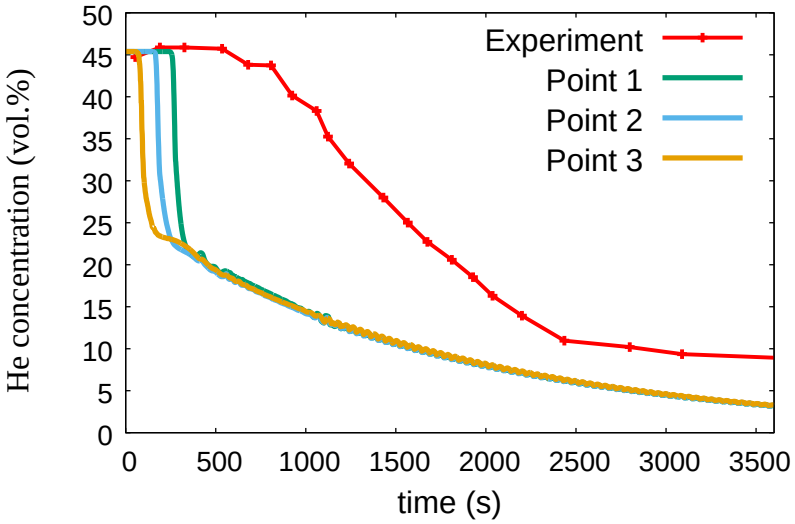

Figure 7. Time-dependent He concentration with corrected (low) lower boundary of He layer (only a single experimental curve is shown).

An additional simulation was performed with a homogenous He-air mixture, with no concentration gradient (Figure 5). In this simulation, erosion also started at first at lowest point 3 and the latest at the highest point 1 (Figure 8). The erosion start, and the initial erosion rate in the point 1 predicted by simulation, match the experimental results, although the erosion rate (that is, the rate of concentration decrease) does not change gradually through the whole simulation but more stepwisely. The He layer erosion obtained with a homogeneous atmosphere was also non-homogeneous, contrary to the experiment.

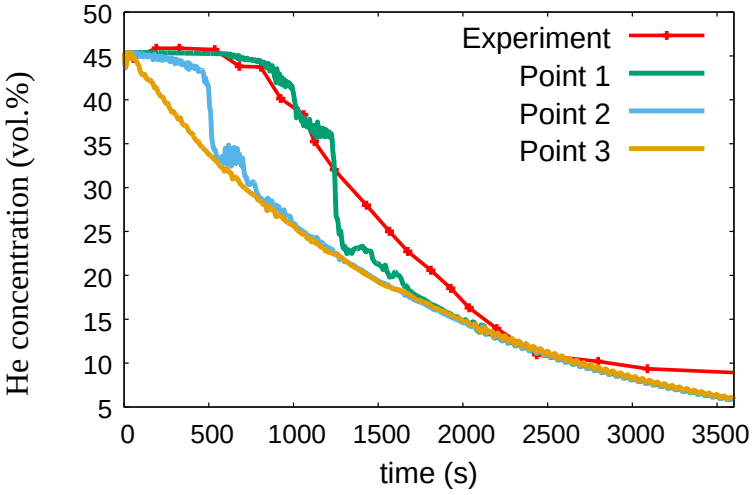

Figure 8. Time-dependent He concentration with homogenous He layer (only a single experimental curve is shown).

6.3. On the Vessel Shape Effect

In Figure 3, it can be observed that the He concentration in the beginning of the experiment is the same in all three measuring points. The experimentalists tried to perform the experiment at similar conditions

as in the PANDA and MISTRA facilities, where the interaction Froude number [5] was 0.75. This means that the jet at the point of interaction with the He layer does not have sufficient momentum to break through all three points simultaneously. Despite the vessel shape differences, the increase of the jet velocity cannot be high enough to increase interaction Froude number up to 2, where the interaction velocity would be high enough to quickly break the layer. Consequently, the erosion process starts lower and gradually progresses upwards, which inhibits the air jet to reach all measuring points simultaneously. This can be also concluded from the time the air jet needs to erode through the layer. Since the time to erosion start is approx. 1000 s (Figure 3), a and there must be other reasons for the observed behaviour of the helium layer. At present, this issue is still open.

One of the possible effects of different shape could be the generation of a recirculation zone stronger than ones created in other facilities (PANDA, MISTRA), which would increase the entrainment to such an extent, that it would neglect the effect of the erosion process, since most of the helium would be constantly returned into the main jet instead of being transported to lower atmosphere regions. This would generate a recirculation zone with same He content in the upper region of the jet. However, the recirculation regions observed in the simulations, where the exact vessel shape is already considered, were not much different from those in the PANDA simulations (ref. [11]), where the entrainment was predicted correctly.

7. CONCLUSIONS

An experiment involving the erosion of a light-gas horizontal layer in the upper part of a cylindrical vessel was simulated with a Computational Fluid Dynamics code, with three different prescribed initial layer configurations. Although simulations provided sensible results, they failed to replicate the specific features of the experiment, namely the slow and homogeneous erosion of the layer. No definitive conclusion as to the reasons for this disagreement has been proposed yet, and the issue will be investigated further.

ACKNOWLEDGMENTS

The experiment was performed within the Chinese-European ALISA (Access to Large Infrastructures for Severe Accidents) project (contract number: 295421, 2014-2018). The work of the Jožef Stefan Institute was performed within the research programme “Reactor Engineering” (P2-0026, 2015-2019).

REFERENCES

1. I. Kljenak, A. Bentaïb, T. Jordan, “Early Containment Failure - Hydrogen Behavior and Control in Severe Accidents”, in: B.R. Sehgal (Ed.), *Nuclear Safety in Light Water Reactors,* Elsevier, pp. 186–227, Elsevier (2012).
2. *OECD/SETH-2 Project PANDA and MISTRA Experiments – Final Summary Report*, NEA/CSNI/R(2012)5, OECD Nuclear Energy Agency (2012).
3. J. Malet, E. Porcheron, J. Vendel, “OECD International Standard Problem ISP-47 on Containment Thermal-Hydraulics—Conclusions of the TOSQAN Part”, *Nuclear Engineering and Design*, **253**, pp. 406-412 (2012).
4. H. Gong, Y. Wang, Y. Zan, P. Li, I. Kljenak, E. Studer, A. Bentaïb, N. Méchitoua, “Experiment on Light Gas Layer Erosion in Small-Scale MCTHBF Containment Experimental Facility,” *Proceedings of 12th International Topical Meeting on Nuclear Reactor Thermal-Hydraulics, Operation and Safety (NUTHOS-12),* Qingdao, China, October 14-18, 2018.
5. E. Studer, J. Brinster, I. Tkatschenko, G. Mignot, D. Paladino, M. Andreani, “Interaction of a Light Gas Stratified Layer With an Air Jet Coming From Below: Large Scale Experiments and Scaling Issues”, *Nuclear Engineering and Design*, **253**, pp. 406-412 (2012).

6. OpenCFD Ltd., "OpenFoam: The open source CFD toolbox", http://www.openfoam.com/, view: 16.08.2016
7. B. E. Launder, D. B. Spalding, "The Numerical Computation of Turbulent Flows", *Computer Methods in Applied Mechanics and Engineering*, **3**, pp. 269-289 (1974).
8. R. A. W. M. Henkes, F. F. van der Flugt, C. J. Hoogendoorn, "Natural-Convection Flow in a Square Cavity Calculated with Low-Reynolds-Number Turbulence Models", *International Journal of Heat and Mass Transfer*, **34**, pp. 377-388 (1991).
9. M. F. Modest, *Radiative Heat Transfer (Third Edition)*, Academic Press, Boston, Massachusetts (2013).
10. M. N. Ozisik, *Radiative Transfer and Interactions with Conduction and Convection*, Wiley, New York (1973).
11. R. Krpan, I. Kljenak, "Simulation of PANDA SETH2 Experiments on Containment Atmosphere Mixing Caused by Vertical Injection", *OECD/NEA&IAEA, Application of CFD/CMFD Codes to Nuclear Reactor Safety and Design and their Experimental Validation Workshop*, Shanghai, China, September 4-6, 2018.